Author/s:
Tran, LS;Tran, D;De Paoli, A;D'Costa, K;Creed, SJ;Ng, GZ;Le, L;Sutton, P;Silke, J;Nachbur, U;Ferrero, RL

Title:
NOD1 is required for Helicobacter pylori induction of IL-33 responses in gastric epithelial cells

Date:
2018

Citation:
Tran, L. S., Tran, D., De Paoli, A., D'Costa, K., Creed, S. J., Ng, G. Z., Le, L., Sutton, P., Silke, J., Nachbur, U. & Ferrero, R. L. (2018). NOD1 is required for Helicobacter pylori induction of IL-33 responses in gastric epithelial cells. Cellular Microbiology, 20 (5), https://doi.org/10.1111/cmi.12826.

Persistent Link:
https://hdl.handle.net/11343/283625

Ferrero Richard (Orcid ID: 0000-0002-5382-3903)

NOD1 is required for *Helicobacter pylori* induction of IL-33 responses in gastric epithelial cells

Le Son Tran[1,], Darren Tran[1], Amanda De Paoli [1], Kimberley D'Costa[1], Sarah J. Creed[2], Garrett Z. Ng[3,4], Lena Le[1], Philip Sutton[3,4,5], J. Silke[6,7], U. Nachbur[6,7], Richard L. Ferrero[1,8,*]*

[1] Centre of Innate Immunity and Infectious Diseases, The Hudson Institute of Medical Research, Monash University, 27-31 Wright Street, Clayton, Victoria, Australia;

[2] Monash Micro Imaging, The Hudson Institute of Medical Research, Monash University, 27-31 Wright Street, Clayton, Victoria, Australia;

[3] Murdoch Children's Research Institute, The Royal Children's Hospital, 50 Flemington Road, Parkville, Victoria, Australia;

[4] School of Veterinary and Agricultural Science, The University of Melbourne, Corner Park Drive and Flemington Road, Parkville, Victoria 3010, Australia;

[5] Department of Paediatrics, The University of Melbourne, Parkville, Victoria 3010, Australia;

[6] Division of Cell Signalling and Cell Death, The Walter and Eliza Hall Institute, 1G Royal Parade, Parkville, Victoria, Australia;

[7] Department of Medical Biology, The University of Melbourne, Parkville, Victoria 3010, Australia;

[8] Biomedicine Discovery Institute, Department of Microbiology, Monash University, 23 Innovation Walk, Clayton, Victoria, Australia.

[*] **Corresponding authors:**

This is the author manuscript accepted for publication and has undergone full peer review but has not been through the copyediting, typesetting, pagination and proofreading process, which may lead to differences between this version and the Version of Record. Please cite this article as doi: 10.1111/cmi.12826

Dr Le Son Tran; Email: leson.tran@hudson.org.au; Tel: +61 3 99024713

A/Prof. Richard Ferrero; Email: richard.ferrero@hudson.org.au; Tel: +61 3 85722728

Running title: *H. pylori* regulation of IL-33 responses

SUMMARY

Helicobacter pylori causes chronic inflammation which is a key precursor to gastric carcinogenesis. It has been suggested that *H. pylori* may limit this immunopathology by inducing the production of IL-33 in gastric epithelial cells, thus promoting T helper 2 immune responses. The molecular mechanism underlying IL-33 production in response to *H. pylori* infection, however, remains unknown. In the current study, we demonstrate that *H. pylori* activates signalling via the pathogen recognition molecule NOD1 and its adaptor protein RIPK2, to promote production of both full-length and processed IL-33 in gastric epithelial cells. Furthermore, IL-33 responses were dependent on the actions of the *H. pylori* type IV secretion system (T4SS), required for activation of the NOD1 pathway, as well as on the T4SS effector protein, CagA. Importantly, *Nod1*$^{+/+}$ mice with chronic *H. pylori* infection exhibited significantly increased gastric IL-33 and splenic IL-13 responses, but decreased IFN-γ responses, when compared with *Nod1*$^{-/-}$ animals. Collectively, our data identify NOD1 as an important regulator of mucosal IL-33 responses in *H. pylori* infection. We suggest that NOD1 may play a role in protection against excessive inflammation.

1. INTRODUCTION

Chronic inflammation caused by infection with the Gram-negative bacterium *Helicobacter pylori* is an essential precursor to gastric carcinogenesis [1]. Upon infection, *H. pylori* interacts with host cells within the gastric mucosa, resulting in activation of multiple innate immune signalling pathways that shape host adaptive immune responses [2]. Innate immune recognition of *H. pylori* results in T helper (Th) 1 and 17 responses which promote the development of gastric immunopathologies [3, 4]. It has been shown, however, that *H. pylori* can limit excessive gastric inflammation and promote bacterial persistence through the induction of Th2 immune responses [5-7].

The IL-1 cytokine family comprises 11 members and has been described as important drivers of the host adaptive cytokine profile [8]. A recently identified member of this family, IL-33, has been shown to act as an alarmin and be associated with Th2 signature cytokine production (*e. g*. IL-4, IL-5 and IL-13) by group 2 innate lymphoid cells and Th2 lymphocytes during allergic inflammation or parasite infection [9]. In addition, IL-33 was shown to promote the proliferation of regulatory T cells and to function as an anti-inflammatory cytokine mediating tissue repair [10, 11].

A recent study reported upregulated *IL33* gene expression in human gastric mucosa in response to *H. pylori* infection [12]. Buzzelli *et al.* [13] demonstrated increased IL-

33 responses in the gastric mucosa of *H. pylori*-infected mice in the acute phase of infection, whereas its expression was reduced during chronic infection. Despite the observed association between *IL33* expression and *H. pylori* infection, the upstream signalling mechanism underlying *H. pylori* regulated IL-33 production remains elusive.

We have previously reported that the cytosolic receptor Nucleotide-Binding Oligomerisation Domain-Containing protein 1 (NOD1) is an important pathogen recognition receptor (PRR) regulating host epithelial cell responses to *H. pylori* [14]. NOD1 was shown to sense Gram-negative peptidoglycan (PG), delivered into the cytoplasm of host cells via the *H. pylori* type IV secretion system, encoded by the *cag* pathogenicity island (CagPAI) [14-16]. In addition to the T4SS, *H. pylori* can activate the NOD1 pathway via the actions of outer membrane vesicles (OMVs) which function as a transport mechanism for bacterial PG into the host cell cytosol [17-19]. Upon recognition of PG, NOD1 undergoes self-oligomerisation, leading to the recruitment of the scaffolding kinase protein, receptor-interacting serine-threonine kinase 2 (RIPK2; also known as RIP2, RICK or CARDIAK) [15, 19-21]. This leads to activation of nuclear factor-kappa B (NF-κB) and mitogen-activated protein kinases (MAPK) signalling pathways and the subsequent transcriptional activation of multiple pro-inflammatory cytokine genes [15].

Given that IL-33 is downstream of the NF-κB signalling pathway [22, 23], we hypothesised that NOD1 sensing of *H. pylori* infection may regulate IL-33 responses in the stomach. Here, we show that NOD1 is required for *H. pylori* upregulation of IL-

33 gene expression, synthesis and processing in gastric epithelial cells *in vitro* and *in vivo*. Furthermore, NOD1 regulation of IL-33 production was shown to be associated with the development of Th2-type immune responses in mice with chronic *H. pylori* infection, suggesting a protective role for NOD1 against excessive inflammation.

2. RESULTS

2.1 NOD1 sensing of *H. pylori* mediates IL-33 responses in gastric epithelial cells

It has been shown that IL-33 production is mediated by NF-κB signalling and that sensing of *H. pylori* infection by NOD1 leads to the activation of NF-κB signalling in gastric epithelial cells [14, 15, 22, 23]. In order to initially investigate the link between NOD1 signalling and IL-33 regulation in response to *H. pylori*, we used the mouse GSM06 gastric epithelial cell line. To block NOD1 signalling in GSM06 cells, we pre-treated cells with the NOD1-specific inhibitor ML130 [24]. As expected, inactivation of NOD1 signalling by treatment with ML-130 significantly attenuated the production of KC, a cytokine downstream of *H. pylori* induced NOD1 activation (**Figure 1a**; $p < 0.01$). Likewise, the stimulation of cells with *H. pylori* bacteria induced upregulated *Il33* gene expression and this was significantly reduced in cells pre-treated with ML130 (**Figure 1b**; $p=0.03$). Consistent with the gene expression

data, full-length IL-33 (33 kDa) production was increased in the lysates of GSM06 cells in response to *H. pylori* stimulation, whereas the levels were reduced when NOD1 signalling was inhibited by ML130 treatment (**Figure 1c**). Furthermore, we detected higher levels of processed IL-33 (22 kDa) in the lysates and culture supernatants of GSM06 cells following *H. pylori* stimulation as compared with ML130-treated cells (**Figure 1c**). Lower levels of total IL-33 were also detected in the culture supernatants of ML-130-treated GSM06 cells, as compared with control cells **(Figure S1e)**. These data showed that NOD1 promotes both gene transcription and protein production of IL-33 in mouse gastric epithelial cells. To further investigate the contribution of NOD1 in IL-33 regulation, we isolated primary mouse gastric epithelial cells (GEC) from *Nod1*$^{+/+}$ or *Nod1*$^{-/-}$ mice. The purity of the GEC preparations was confirmed by immunofluorescence staining with an antibody to the epithelial cell specific marker, EpCAM (**Figure S1a,b**). The reduction in KC and MIP2 production in *Nod1*$^{-/-}$ GECs further confirmed the important role of NOD1 in activation of NF-κB in response to *H. pylori* stimulation (**Figure S1c,d**). The GECs were then co-cultured with the *H. pylori* clinical strain 10700 or its mouse-adapted variant, Sydney strain 1 (SS1). Consistent with findings in GSM06 cells, the levels of full-length and processed IL-33 were markedly lower in *Nod1*$^{-/-}$ GECs as compared with *Nod1*$^{+/+}$ cells in response to either 10700 or SS1 stimulation (**Figure 1d**). To extend our findings, we used human AGS GEC lines, stably expressing a shRNA specific for *NOD1* or an irrelevant gene *EGFP* (hereafter referred to as sh.*NOD1* AGS or sh.*EGFP*, respectively [25]). Increased levels of *IL33* gene expression, as well as

full-length IL-33 synthesis and processing, were observed in sh.*EGFP* AGS cells in response to stimulation with *H. pylori* 26695 bacteria (**Figure 1e,f**). In contrast, these responses were completely ablated in sh.*NOD1* AGS cells (**Figure 1e,f**). To investigate the role of NOD1 sensing of bacterial PG in IL-33 responses, we stimulated AGS cells with wild type or isogenic mutant bacteria that lack the lytic transglycosylase, Slt (HP0645). These *slt*$^{-}$ mutant bacteria release less NOD1 ligand and therefore also have a reduced capacity to activate the NOD1 signalling pathway [14]. AGS cells that were co-cultured with *H. pylori slt*$^{-}$ bacteria exhibited reduced IL-33 responses when compared with the parental strain (**Figure 1e,f**). Furthermore, *H. pylori* OMVs harbouring PG induced higher levels of full-length and processed IL-33 in sh.*EGFP* AGS cells when compared with sh.*NOD1* cells (**Figure S2**). These findings confirm the importance of NOD1 sensing of *H. pylori* PG for IL-33 responses in GECs.

To confirm our findings, we generated *NOD1* knockout (KO) AGS cells using CRISPR/Cas9 technology to target the CARD domain of NOD1, which is required for its interaction with downstream adaptor molecules and activation of NF-κB signalling [26]. The isolated *NOD1* KO clone#1 and clone#2 were shown to carry 71-bp and 31-bp deletions, respectively, introducing premature stop codons that resulted in truncated proteins (**Figure S3a and S3b**). As expected, the two knockout clones displayed undetectable levels of *NOD1* gene expression (**Figure S3c**) and attenuated IL-8 production in response to NOD1 agonist C12-EiDAP or *H. pylori* stimulation (**Figure S3d**). Importantly, both *NOD1* KO AGS clones express

significant lower levels of *IL33* gene expression (**Figure 1g**, $p = 0.03$) and produce less full-length and mature IL-33 protein than control AGS cells (**Figure 1h**). Taken together, these findings show that activation of NOD1 signalling by *H. pylori* enhances IL-33 production in both mouse and human GECs.

In addition to NOD1, recent studies have reported that the host tumor necrosis factor receptor-associated factor (TRAF)-interacting protein with forkhead-associated domain (TIFA) drives NF-κB activation upon detection of heptose-1,7-bisphosphate (HBP), an intermediate product of LPS biosynthesis [27-29]. To address the contribtion of TIFA in *H. pylori*-induced IL-33 production, we "knocked down" its expression by transfecting AGS cells with *TIFA*-specific siRNA prior to bacteria stimulation. Transfection with *TIFA* siRNA resulted in significant reductions in *TIFA* gene expression and IL-8 responses (**Figure S4a,b**), yet the levels of both full-length and mature forms of IL-33 in the lysates of *H. pylori*-stimulated cells remained unchanged **(Figure S4c)**. Interestingly, AGS cells in which *TIFA* expression was reduced by siRNA treatment secreted lower levels of mature IL-33 into the culture supernatants, as compared with control AGS cells **(Figure S4c)**. These data suggest that unlike NOD1, TIFA is required for IL-8 production and in proteolytic processing of full-length IL-33, but is dispensable for IL-33 synthesis.

2.2 RIPK2 is required for NOD1-mediated production and processing of IL-33

RIPK2 has been described to be a central down-stream mediator of NOD1 signalling [21]. To test the role of RIPK2 in *H. pylori*-mediated IL-33 responses, AGS cells were

either transfected with *RIPK2*- specific siRNA or pre-treated with the RIPK2 inhibitor, WEHI-345, prior to *H. pylori* stimulation [30]. siRNA-mediated knock down of *RIPK2* expression was confirmed by qPCR (**Figure 2a**; p=0.03). Additionally, inhibition of RIPK2 function was confirmed by measuring IL-8 responses as the production of this chemokine in response to *H. pylori* stimulation is known to be NOD1-dependent (**Figure 2b,c**). Importantly, RIPK2 inhibition resulted in reduced levels of IL-33 production and processing (**Figure 2d,e**). These data show that classical NOD1/RIPK2 signalling is important in mediating the IL-33 responses induced by *H. pylori*.

2.3 Loss of nuclear localisation of IL-33 in response to *H. pylori* stimulation is NOD1-dependent

It has been reported that under basal conditions, IL-33 predominantly resides in the nucleus of epithelial cells, whereas loss of its nuclear location is associated with enhanced release of IL-33 and induction of inflammatory responses [31, 32]. Consistent with the published literature, IL-33 expression was predominantly localised within the nucleus of unstimulated control and *NOD1* KO AGS cells (**Figure 3a,b**). *H. pylori* stimulation promoted the re-localisation of IL-33 from the nucleus to the cytoplasm in control cells, but not in *NOD1* KO AGS cells, which instead displayed a predominantly nuclear localisation for IL-33 similar to that in non-stimulated cells (**Figure 3c,d**). This observation was further confirmed by a significant reduction in the ratio of nuclear to cytoplasmic IL-33 in control cells, but

not in *NOD1* KO AGS cells after stimulation with *H. pylori* (**Figure 3e**, p = 0.0005). These data indicate that NOD1 is involved in promoting the nuclear release of IL-33. Thus, NOD1 not only promotes the synthesis of IL-33 protein but also release of this cytokine, which may allow host epithelial cells to activate other immune cell subsets and shape the downstream immune responses to *H. pylori* infection.

2.4 The *H. pylori* T4SS and CagA are required for induction of IL-33 in human GECs.

The *H. pylori* T4SS is one mechanism by which bacteria can deliver their PG into the cytoplasm of host cells, leading to the activation of NOD1 signalling [14]. Therefore, we addressed whether bacterial T4SS plays a role in NOD1-mediated IL-33 responses by co-culturing human AGS cells with wild type *H. pylori* 251 or isogenic mutant strains having either defective T4SSs (*i. e.* Δ*cag*PAI, Δ*cagM*) or lacking the T4SS effector protein, CagA (Δ*cagA*). These mutant *H. pylori* bacteria induced significantly reduced levels of IL-8 production when compared with wild type bacteria (**Figure 4a**; p<0.05). *H. pylori* mutant bacteria with defective T4SSs also induced significantly lower levels of *IL33* expression (**Figure 4b**; p=0.03), as well as reduced production of both full-length and processed IL-33 (**Figure 4c,d**; p=0.03). Interestingly, *H. pylori* Δ*cagA* bacteria also induced significantly reduced IL-33 responses in AGS cells (**Figure 4c,d**; p=0.03). Taken together, our data show that T4SS, which is required for the activation of NOD1 signalling, as well as for

translocation of the CagA oncoprotein, contributes to *H. pylori* induced IL-33 production in human GECs.

2.5 NOD1 drives IL-33 production and Th2 cytokine responses during chronic *H. pylori* infection *in vivo*

To study the role of NOD1 in IL-33 production *in vivo*, *Nod1*$^{+/+}$ and *Nod1*$^{-/-}$ mice were inoculated with *H. pylori* and left for 1 or 8 weeks, respectively. At 1 week post-infection, we observed no significant changes in *Il33* gene expression (**Figure 5a**) or IL-33 production (**Figure 5b**) in the stomachs of either *H. pylori*-infected *Nod1*$^{+/+}$ or *Nod1*$^{-/-}$ mice, when compared with control uninfected animals. In contrast, at 8 weeks post-infection *Nod1*$^{-/-}$ animals displayed significantly down-regulated levels of *Il33* gene expression (**Figure 5a**; p=0.01) and protein production (**Figure 5b**; p=0.0002), when compared with *H. pylori*-infected *Nod1*$^{+/+}$ animals. The former also exhibited lower levels of both full-length and processed IL-33 forms (**Figure 5c**). Thus, consistent with our *in vitro* data, NOD1 mediates IL-33 production during chronic infection with *H. pylori.*

Given that IL-33 is a key driver of Th2 immunity in a wide range of inflammatory settings, we next investigated the cytokine profiles of splenocytes isolated from *Nod1*$^{+/+}$ or *Nod1*$^{-/-}$ mice at 8 weeks post-infection. Although splenocytes from *Nod1*$^{+/+}$ and *Nod1*$^{-/-}$ mice produced similar levels of the Th2 cytokines, IL-4 and IL-10, significant differences were observed for another Th2 cytokine, IL-13 (**Figure 5d-f**; *p=0.03*). Conversely, the splenocytes from *Nod1*$^{-/-}$ mice produced significantly higher

levels of the Th1 cytokine IFN-γ, as compared with *Nod1*$^{+/+}$ splenocytes (**Figure 5g**; *p*=0.03). No differences were observed for the Th-17 cytokine, IL-17 (**Figure 5h**). Thus, during chronic infection with *H. pylori*, NOD1 is involved in IL-33 production thereby shaping host adaptive immune responses towards a Th2-dominant phenotype.

3. Discussion

IL-33 is well established as an important mediator of both innate and adaptive immune responses [11]. Although recent studies have revealed an association between mucosal IL-33 production and *H. pylori* infection, the underlying mechanism by which the bacterium drives IL-33 production remains unknown [12, 13]. In this study, we show that *H. pylori* activation of the innate immune molecule NOD1 promotes *IL33* gene expression and processing in GECs.

It has recently been reported that IL-33 induction is driven by NF-κB signalling in epithelial cells in response to bacterial infection and inflammation [22, 23]. This led us to hypothesise that in response to *H. pylori* infection, NOD1 may regulate IL-33 production in epithelial cells. Consistent with this hypothesis, we showed that disruption of NOD1 signalling by either pharmacological inhibition, siRNA knockdown or CRISPR/Cas9 gene targeting resulted in attenuation of both classical NF-κB-dependent cytokine production and IL-33 responses. Furthermore, we showed that blockade of RIPK2, a critical downstream mediator of NOD1 signalling responsible for NF-κB activation [33], resulted in decreased IL-33 production. Thus, these findings suggest that NOD1 sensing of *H. pylori* promotes IL-33 production via activation of the NF-κB signalling pathway.

It is thought that IL-33 possesses a nuclear localisation sequence within its N terminus and is thus normally stored in the nucleus in order to be protected from cleavage and inappropriate release [34, 35]. In this study, we observed that NOD1 activation by *H. pylori* caused loss of nuclear IL-33 and enhanced secretion of

processed IL-33 in the culture supernatants of control AGS cells, but not those from *NOD1* KO cells (**Figure 3**). Thus, it is possible that NOD1 mediates the release of IL-33 via cleavage of an N-terminal nuclear localisation signal required for tethering IL-33 in the nucleus. However, the mechanism(s) whereby these processed forms are secreted into the extracellular compartment remain(s) largely unknown. The processed form of IL-33 may be biologically active or inactive, depending on the proteases mediating the cleavage [11]. In common with other members of the IL-1 cytokine family, IL-33 was initially reported to become active after processing by caspase-1 [36]. However, subsequent studies showed that caspase-1 and other apoptotic caspases, including caspases-3 and -7, could cleave IL-33 into an inactive form [37]. IL-33 can also be processed by neutrophil proteases, resulting in highly active forms [38]. Thus, future studies are needed to assess the protease(s) responsible for the processing of IL-33 in GECs, the secretion mechanism involved in release of the processed form, as well as the role of NOD1 in IL-33 processing and its impact on *H. pylori*-induced pathology.

The turnover and release of PG mediated by the lytic transglycosylase. Slt, has been shown to be important for *H. pylori* to activate NOD1 signalling [14]. In the present study, we show that AGS cells stimulated with *H. pylori slt* deficient bacteria induced significantly lower levels of IL-33 mRNA and protein than those stimulated with wild type bacteria (**Figure 1e,f**). These data suggest the importance NOD1 sensing of PG in IL-33 responses. Consistent with this suggestion, *H. pylori* OMVs induced IL-33 responses via a NOD1-dependent mechanism (**Figure S2**). In

addition, *H. pylori* mutant bacteria lacking a functional T4SS system, which is required to activate NOD1 signalling via the delivery of PG into host cells [14], were affected in their ability to induce IL-33 responses in human GECs (**Figure 4**). It is also noteworthy that we observed higher levels of processed IL-33 in the culture supernatants of mouse GECs after stimulation with the clinical isolate 10700, which has a functional T4SS, when compared with those from cells stimulated its mouse-adapted variant (strain SS1), which lacks a functional T4SS [39] (**Figure 1d**). Although the T4SS is not essential for *H. pylori* induction of NF-κB-dependent responses in mouse GECs [40], it is possible that this secretion system may be required for maximal IL-33 responses in GECs of murine origin. Altogether, these data suggest that the metabolism and delivery of PG into host cells are crucial for *H. pylori* activation of NOD1-driven IL-33 responses in GECs.

The induction of both IL-8 and IL-33 production was not completely abrogated in GECs in which NOD1 signalling had been dampened by either pharmacological inhibition, shRNA knockdown or gene deletion (**Figure 1c, e-h**), suggesting the potential involvement of a NOD1-independent mechanism in these responses. Although the contribution of CagA in *H. pylori* induced NF-κB responses remains controversial, we found that *H. pylori* Δ*cagA* bacteria induced less IL-8 production compared with wild type bacteria and, moreover, these responses were not completely abolished in sh.*NOD1* AGS cells (**Figure 5a**). Additionally, we showed that *H. pylori* Δ*cagA* bacteria induced lower levels of IL-33 production and processing (**Figure 4c,d**), suggesting that CagA may act independently of NOD1 signaling to

drive IL-33 production. Although beyond the scope of the current study, the mechanism whereby *H. pylori* CagA regulates IL-33 responses warrants further investigation.

Unlike NOD1, we found that TIFA is dispensable for the production of full-length IL-33 in cell lysates. IL-33 is known as an “alarmin” which is released rapidly during the early phase of infection to alert the host immune system to the presence of bacteria [10]. We speculate that NOD1 is the first sensor recruited to the cell membrane upon initial contact with *H. pylori*, hence predominantly mediating a rapid response. This speculation is supported by a recent study by Gaudet *et al.* [27] showing that NOD1 and TIFA independently contribute to NF-κB activation by the invasive Gram-negative bacterium, *Shigella flexneri*, and that the activation of NOD1 pathway precedes TIFA. In contrast, however, Gall *et al.* [28] claimed that in *H. pylori* infection, TIFA is activated prior to the NOD1 response. Nevertheless, there is currently no experimental evidence to support this sequential activation of NOD1 and TIFA during *H. pylori* infection. Future studies are therefore required to delineate the links between NOD1 and TIFA activation during *H. pylori* stimulation. Interestingly, a reduction in the levels of mature IL-33 was observed in the culture supernatants of cells in which *TIFA* had been knocked down using siRNA (Figure S4c). Thus, the involvement of both NOD1 and TIFA in IL-33 processing indicates that these proteins might be components of a protein complex that mediates proteolytic cleavage of IL-33 at later phases of infection.

To establish the *in vivo* significance of NOD1-mediated IL-33 production, we assessed IL-33 production in both the acute and chronic phases of infection (1 and 8 weeks' post-infection). In line with a recent clinical study that reported a strong correlation between chronic *H. pylori* infection and *IL33* gene expression in human gastric biopsies [12], we found enhanced IL-33 production in the chronic phase of infection (**Figure 5a-c).** A recent study by Buzzelli *et al.* [13], however, reported that *IL33* gene expression was increased in the early phase of infection (1 week) but reduced after long term infection. This discrepancy could be attributed to differences in the *H. pylori* strains used in the two studies. Indeed, Buzzelli *et al.* used the *H. pylori* SS1 strain that was previously shown to have lost its T4SS functions during *in vivo* colonization [39]. In contrast, we used the *H. pylori* 245m3 strain in our study which has an intact *cag*PAI and still possesses a functional T4SS (L. S. Tran, K. D'Costa, unpublished data). It is possible that this allows the bacterium to sustain IL-33 production during long term infection.

Importantly, the levels of gastric IL-33 mRNA and protein were significantly higher in *Nod1*$^{+/+}$ than *Nod1*$^{-/-}$ mice (**Figure 5a,b**). These IL-33 responses were associated with up-regulation of IL-13 and down-regulation of IFN-γ in splenic lymphocytes (**Figure 5d,g**). Based on previous findings [3, 41], these responses would be expected to attenuate the development of gastric inflammation and affect bacterial clearance. One possible mechanism underlying the beneficial effects of IL-33 is that this cytokine can drive the generation of regulatory T cells which was reported to limit inflammatory responses and reduce bacterial loads in mice infected with *H. pylori*

[42]. In contrast, IL-33 was shown to elicit Th1 immune responses in tumor tissues by inducing IFN-γ production in $CD8^+$ T cells and NK cells [43]. Thus, future studies should explore the biological consequences of IL-33 production in the context of *H. pylori* infection and disease.

Collectively, in this work, we report for the first time that *H. pylori* infection promotes IL-33 secretion in GECs via a NOD1-dependent mechanism. Additionally, NOD1-driven IL-33 production during chronic *H. pylori* infection is associated with a Th2-type immune response, which may protect against excessive inflammatory responses and favour the persistence of *H. pylori* infection.

Experimental procedures

Cell lines, bacterial and mouse strains

The mouse GSM06 GEC line (RCB1779) was obtained from Riken Cell Bank and grown as described previously [40]. Briefly, the cells were maintained in Dulbecco's modified Eagle medium–nutrient mixture/F-12 medium, supplemented with 10% FCS, 1% (w/v) insulin/transferring/selenite (Gibco) and 10 ng/ml epidermal growth factor. Cells were grown in 5% CO_2 at the permissive temperature of 33˚C, then moved to 37˚C prior to experiments.

Human AGS gastric cancer cells stably expressing sh.RNA to either *EGFP* (sh.*EGFP*) or *NOD1* (sh.*NOD1*) were generated as described previously [25]. These cells were maintained in complete RPMI medium supplemented with 10% (v/v) foetal calf serum (FCS), 1% (w/v) L-glutamine and 1 % (w/v) penicillin/streptomycin (Gibco; ThermoFisher Scientific, VIC, Australia).

AGS cells harbouring CRISPR/Cas9 mediated *NOD1* gene knockout were generated by using a "Cas9 nickase" nuclease with pairs of guide RNAs (gRNAs) to introduce double-strand breaks [44]. The following pair of gRNAs were designed to target the CARD domain of NOD1: gRNA1: GCTGAAGAATGACTACTTC and gRNA2: GCTTTTCAGTAATTGAATGT. These gRNAs were cloned into pSpCas9n(BB)-2A-GFP (PX461) (Addgene plasmid # 48140) and pSpCas9n(BB)-2A-Puro (PX462) (Addgene plasmid # 48141). The ligated vectors were transfected into AGS cells using Lipofectamine LTX (ThermoFisher Scientific) and then cells were selected with 1 μg/ml puromycin. As a control, cells were transfected with PX461 and PX462

plasmids not carrying gRNAs. Limiting dilution was performed to obtain mutant clones derived from a single cell. Frame-shift knockout clones were screened by PCR and pyrosequencing with primers flanking the target region: Fwd-GGCCACAGTGAGATGGAAAT and Rev- GGCAGGCACACACAATCTC. The knock out status of *NOD1* in AGS cells was further verified by measuring the levels of *NOD1* gene expression and NOD1 induced IL-8 production in response to NOD1 agonist C12-iEDAP (10 μg/ml, Invivogen).

H. pylori strains 26695 (wild type, *slt*$^-$) [14], 251 (wild type, *cagM*$^-$, *cag*PAI$^-$, *cagA*$^-$) [15], Sydney strain 1 (SS1) and 10700 [45] were used for *in vitro* experiments. A mouse-adapted, *cag*PAI$^+$ *H. pylori* strain (245m3) [39] was employed for *in vivo* experiments. All bacterial strains were grown on Blood Agar Base No. 2 (Oxoid; Thermo Fisher Scientific), supplemented with 5% (v/v) whole horse blood (Australian Ethical Biologicals, VIC, Australia), Skirrow's selective supplement (155 μg/ml polymyxin B, 6.25 μg/ml vancomycin, 3.125 mg/ml trimethoprim and 1.25 mg/ml amphotericin B; Sigma, MO, USA), at 37˚C under microaerobic conditions.

Nod1$^{+/+}$ and *Nod1*$^{-/-}$ C57BL/6 mice were maintained under specific pathogen-free conditions at the Animal Research Facility (Monash Medical Centre). All animal procedures complied with guidelines approved by Monash Medical Centre Animal Ethics Committee (MMCA/2015/43).

Primary GEC isolation

Stomachs were removed from 4-5 week old *Nod1*$^{+/+}$ or *Nod1*$^{-/-}$ mice and the gastric tissues excised and finely minced in 5 ml of Hank's Balanced Salt Solution without Ca^{2+} and Mg^{2+} (Gibco), supplemented with 0.125% (w/v) bovine serum albumin (Sigma), 0.072% (w/v) dispase (Roche Life Science, NSW, Australia) and 0.1% (w/v) collagenase A (Roche). Tissues were digested by incubation for 2 hrs at 37˚C, in 5% CO_2 and shaking at 150 rpm. Digested tissues were pelleted and washed in DMEM/F12 medium by centrifugation at 300 x *g* for 5 min. Cells were plated at 10^5 cells/ml per well in 24-well plates coated with 2 mg/ml rat Tail Collagen I (ThermoFisher Scientific). The culture medium was changed every 2 days to remove fibroblasts and epithelial cells were grown for 5 days before performing co-culture assays. Epithelial cell purity was confirmed by immunofluorescence using the epithelial cell-specific marker, EpCAM (Abcam, Cambridge, UK, 1:200) and isotype control rabbit IgG (Dako).

OMV isolation

OMVs were purified from mid-exponential phase cultures were pelleted at 4,000 g for 40 min at 4^{o}C (Kaparakis, Cell Micro). Supernatant fractions were collected and filtered through 0.22-µm filters (Merck Millipore, VIC, Australia). Filtered supernatants were subjected to ultracentrifugation as described previously (Kaparakis, Cell Micro). Supernatants were discarded and the pellets resuspended in Brain Heart Infusion medium (Thermo Fisher Scientific). OMV protein concentrations were quantified using the Bradford Protein Assay (BioRad, CA, USA).

Inhibitor treatment

The small molecule inhibitor, ML130 (CID-1088438) was purchased from Tocris (Bristol, UK) and has been confirmed to selectively inhibit NOD1 signaling (IC_{50}= 0.56 μM) with no cytotoxicity in previous studies [24]. The RIPK2 selective inhibitor WEHI-345 was used as described previously [30]. Briefly, cells were pre-treated with ML130 (5 μM) or WEHI-345 (0, 5 or 10 μM) for 1 hr prior stimulation with *H. pylori*, and then maintained in inhibitor-containing medium throughout the experiment process.

siRNA transfection

TIFA or *RIPK2*-specific silencer and negative control siRNA (40 μmol of each; ThermoFisher Scientific) were diluted in Opti-MEM medium (Gibco) supplemented with 2 μl Lipofectamine® 2000 reagent (Thermo Fisher Scientific). The mixtures were incubated at room temperature for 20 min then added in a drop-wise manner to each well of 12-well plates containing 10^5 AGS cells. Transfected cells were incubated at 37˚C for 24 hrs prior to co-culture with bacteria.

Cell co-culture assay

H. pylori liquid cultures were obtained by growing bacteria in BHI containing 10 % (v/v) heat-inactivated foetal calf serum (Thermo Fisher Scientific) and Skrirrow's selective supplement, in a shaking incubator for 16-18 hrs. Bacteria were pelleted

and washed twice with phosphate-buffered saline (PBS) by centrifugation at 4,000 x g for 10 min at 4°C prior to resuspension in RPMI medium for co-culture assays. Viable counts were performed by serial dilution of bacterial suspensions on horse blood agar plates.

Cells were seeded in 12-well plates at 1 x 10^5 cells/ml and allowed to grow overnight. The culture medium was removed and replaced with serum- and antibiotic-free RPMI medium prior to stimulation with bacteria. Cells were incubated with *H. pylori* wild type or isogenic mutant strains at a multiplicity of infection (MOI) of 10:1. The bacteria were removed after 1 hr. RNA extraction was performed at 4 hrs' post-stimulation, whereas culture supernatants and lysates were collected at 24 hrs' post-stimulation for ELISA and Western blot analyses.

qRT-PCR analyses

RNA was extracted using the PureLink® RNA mini kit (Thermo Fisher Scientific). cDNA was generated from 500 µg of RNA using the Tetro cDNA synthesis kit (Bioline, NSW, Australia), as per the manufacturer's instructions. qPCR reactions consisted of 4 µl of diluted synthesised cDNA (1:10), 5µl of SYBR® Green qPCR MasterMix (Thermo Fisher Scientific) and 1 µl of oligonucleotide primers (1 µM) for the tested genes. Oligonucleotide sequences were as follows: *Rn18s*, Fwd-GTAACCCGTTGAACCCCATT and Rev-CCATCCAATCGGTAGTAGCG; *RNA18S1*, Fwd-CGGCTACCACATCCAAGGAA and Rev- GCTGGAATTACCGCGGCT; *Il33,*

Fwd- TTCCAACTCCAAGATTTCCCC and Rev- CAGAACGGAGTCTCATGCAG; *IL33*, Fwd- AGTCTCAACACCCCTCAAATG and Rev- CTTTTGTAGGACTCAGGGTTACC; *RIPK2*, Fwd- GCCACCTGAAAACTATGAACC and Rev- CTGCAAAGGATTGGTGACATC. *TIFA,* Fwd- TCGATTCCCCTCGCTCTG and Rev- CCGTCATCTGGAGACAAGTTAC. qPCR assays were performed in an Applied Biosystems™ 7900 Fast Real-Time PCR machine (Thermo Fisher Scientific), using the following program: 50^0C, 2 min, followed by 95˚C, 10 min, then 40 successive cycles of amplification (95˚C, 15 sec; 60˚C, 1 min). Gene expression levels were determined by the Delta-Delta Ct method to measure relative gene expression levels to the *18S rRNA* gene.

Western blot analyses

Cell culture supernatants were harvested and concentrated with StrataClean resin beads (Agilent Technologies, CA, USA), as per the manufacturer's instructions. Cell lysates were prepared using NP-40 lysis buffer (Thermo Fisher Scientific), supplemented with complete protease and phosphatase inhibitors (Roche). Fifty µg of total protein lysate, as determined using the Qubit™ fluorometer (Thermo Fisher Scientific), were resuspended in 30 µl of Laemmli buffer (Thermo Fisher Scientific). All samples were heated at 98˚C for 10 min, loaded onto NuPAGE® 4-12% gels and run at 120 V in 1 X MES buffer (Thermo Fisher Scientific). The separated proteins were transferred onto membranes using the iBlot® transfer system (Thermo Fisher Scientific), as per the manufacturer's instructions. The membranes were blocked

using Odyssey® blocking buffer (Odyssey; LI-COR, NE, USA). Membranes were incubated with 0.5 ng/ml of goat-anti-human IL-33 antibody (clone AF3625; R&D Systems, MN, USA) overnight, at 4˚C. Membranes were then washed in PBS-Tween 0.05% (v/v) and incubated for 2 hrs with 0.67 ng/ml of rabbit-anti-goat secondary antibody-Alexa Fluor® 680 conjugate (Thermo Fisher Scientific). Membranes were washed and developed on the Odyssey Infrared Imaging System (LI-COR). As loading controls, lysate samples were probed with 0.9 ng/ml of rat-anti-human TUBULIN (Rockland, PA, USA), followed by 0.33 ng/ml of goat-anti-rat secondary antibody-Alexa Fluor® 800 conjugate (Thermo Fisher Scientific). The relative intensity figures for all blots are now presented in Supplementary Table 1.

Immunofluorescence

GECs were fixed with 4% (w/v) paraformaldehyde for 15 min, at room temperature. Cells were washed in PBS and incubated in blocking buffer (3% BSA (w/v) and 0.1% (w/v) saponin in PBS). After 1 hr, cells were incubated overnight, at 4^{o}C with 5 μg/ml of goat anti-human IL-33 primary (clone AF3625; R&D Systems). Samples were washed thrice with blocking buffer and incubated with anti-goat Alexa Fluor® 680-conjugated secondary antibody (1:500) for 1 hr. After washing, cell nuclei were stained with Hoechst 33342 (Thermo Fisher Scientific; 1:1000) for 5 min before mounting. Imaging was performed on a confocal microscope (Nikon Instruments Inc., NY, USA). Cytoplasmic to nuclear ratio measurements were carried out in the FIJI image analysis software on a single image plane extracted from the z-stacks

captured by confocal microscopy. All images were captured using the same settings. Images of the cytoplasmic fractions were created by subtracting Hoechst-stained images from IL-33 stained images using the image calculator in FIJI. A threshold was applied to the stained area in the resulting cytoplasmic fraction image. The mean intensity was measured for the area under the threshold. After measuring the intensity, the threshold of the cytoplasmic fraction image was converted to a binary, which was then subtracted from the original IL-33 stained image, using the FIJI image calculator, to generate a nuclear fraction image. A threshold was then applied to the nuclear fraction image and mean intensity measured.

ELISA

Human CXCL8 (BD Biosciences, NSW, Australia) and mouse KC, MIP-2 and IL-33 (DuoSet ELISA kit, R&D Systems) were quantified by ELISA, as per the manufacturers' instructions. Absorbance values were measured at 450 nm with a FLUOStar® Optima microplate reader (BMG Labtech, VIC, Australia). Cytokine levels were determined by linear or 4-parameter fit analysis.

Mouse H. pylori infection

Nod1$^{+/+}$ and *Nod1*$^{-/-}$ mice (6-8 week old) were inoculated via oral gavage with 10^8 colony-forming units of *H. pylori* strain 245m3 [39], using previously described techniques [46]. Bacterial viability and numbers were determined by agar plate dilution [46]. Stomachs and spleens were harvested from these animals at 1 and 8

wks post-infection. Gastric tissues were subjected to homogenisation using a gentleMACS™ Dissociator (Miltenyi Biotec, NSW, Australia). Bacterial infection status was confirmed by bacteriological culture [46]. Gastric homogenates were then centrifuged at 13,000 x g at 4^{o}C and the supernatants collected for analysis by the Qubit™ protein assay (Thermo Fisher Scientific), ELISA and/or Western blotting.

Cytokine production in splenocytes

Spleens were collected from euthanised mice. Single cell suspensions were obtained by grinding through 70 μm cell strainers. Splenocytes were recovered in RPMI complete medium and seeded at 2 x 10^6 cells/ml in 24-well plates. Cells were left untreated or stimulated with 5 μg/ml concanavalin A (ConA; Sigma) then incubated for 3 days at 37˚C in 5% CO2.

ProcartaPlex Multiplex Immunoassays (eBioscience; Thermo Fisher Scientific) were performed according to the manufacturer's instructions to simultaneously quantify the levels of IL-4, IL-10, IL-13, IL-17 and IFN-γ in splenocyte culture supernatants. Briefly, culture supernatants (50 μl) or standards were mixed with 50 μl magnetic beads and incubated overnight at 4^{o}C. After washing thrice with washing buffer, 50 μl of streptavidin-PE was added and incubated with shaking for 30 min at RT. The mixtures were resuspended in 120 μl of reading buffer after washing thrice with wash buffer. Data were acquired on the Luminex® 100/200™ instrument (Bio-Rad, NSW, Australia). The concentrations of each cytokine were calculated using the ProcartaPlex® Analyst 1.0 Software (eBioscience).

Statistical Analyses

GraphPad Prism (GraphPad Software, CA, USA) was used for graph preparation and statistical analyses. For qPCR assays and ELISA, data were analysed by the Mann–Whitney test. Differences were considered statistically significant for $P < 0.05$.

Conflict of interest: The authors have no conflict of interest to declare.

Acknowledgements

This project was funded by the National Health and Medical Research Council (NHMRC) to RLF (project APP1079930). Research at the Hudson Institute of Medical Research, Murdoch Children's Research Institute and Walter and Eliza Hall Institute is supported by the Victorian Government's Operational Infrastructure Support Program. RLF is a Senior Research Fellow of the NHMRC (APP1079904). KDC is supported by an International Postgraduate Scholarship (Monash University Faculty of Medicine, Nursing and Health Sciences) and funding from the Centre for Innate Immunity and Infectious Diseases.

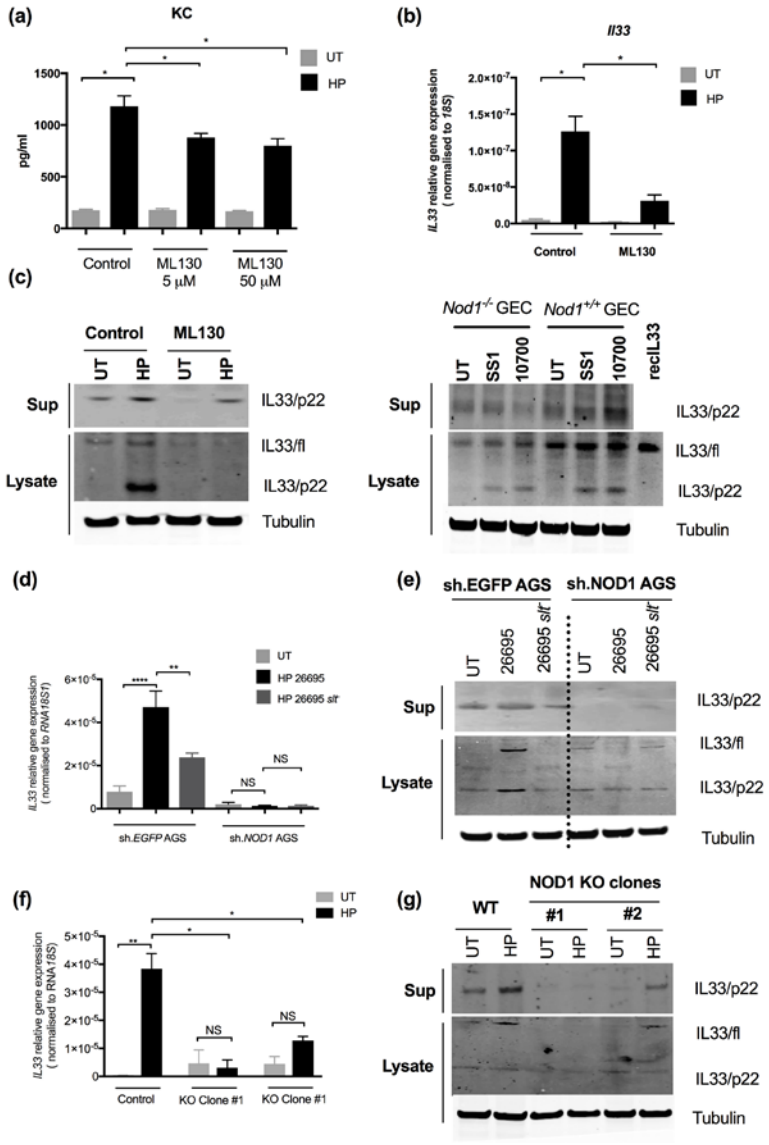

Figure 1. NOD1 sensing of *H. pylori* promotes both full-length and mature IL-33 production in mouse and human GECs.

(a) KC production, (b) *Il33* gene expression and (c) IL-33 protein synthesis in GSM06 mouse GECs pre-treated with NOD1-specific inhibitor ML130 (5 μM), followed by *H. pylori* (HP) stimulation for 6h. (d) Full-length (fl) and processed IL-33 (p22) in primary mouse GECs isolated from *Nod1*$^{+/+}$ *or Nod1*$^{-/-}$ mice infected with *H. pylori* 10700 or SS1. Commercial recombinant IL-33 protein (recIL-33) served as an antibody-specific control. Tubulin was used as a loading control for cell lysates. (e) *IL33* gene expression, (f) Full-length and processed IL-33 in human AGS cells expressing control (sh.*EGFP*) or *NOD1*-specific shRNA (sh.*NOD1*) stimulated with wild type

(26695) or an isogenic mutant (26695 *slt*$^{-}$) at an MOI=10 for 24 hrs. (g) *IL33* gene expression and (h) IL-33 protein production in control or *NOD1* knockout AGS cell lines. Data in (a), (b), (e) and (g) are presented as means ± SEM and are representative of at least two independent experiments (n>2). *p< 0.05, **p<0.01, ***p<0.001, NS= not significant.

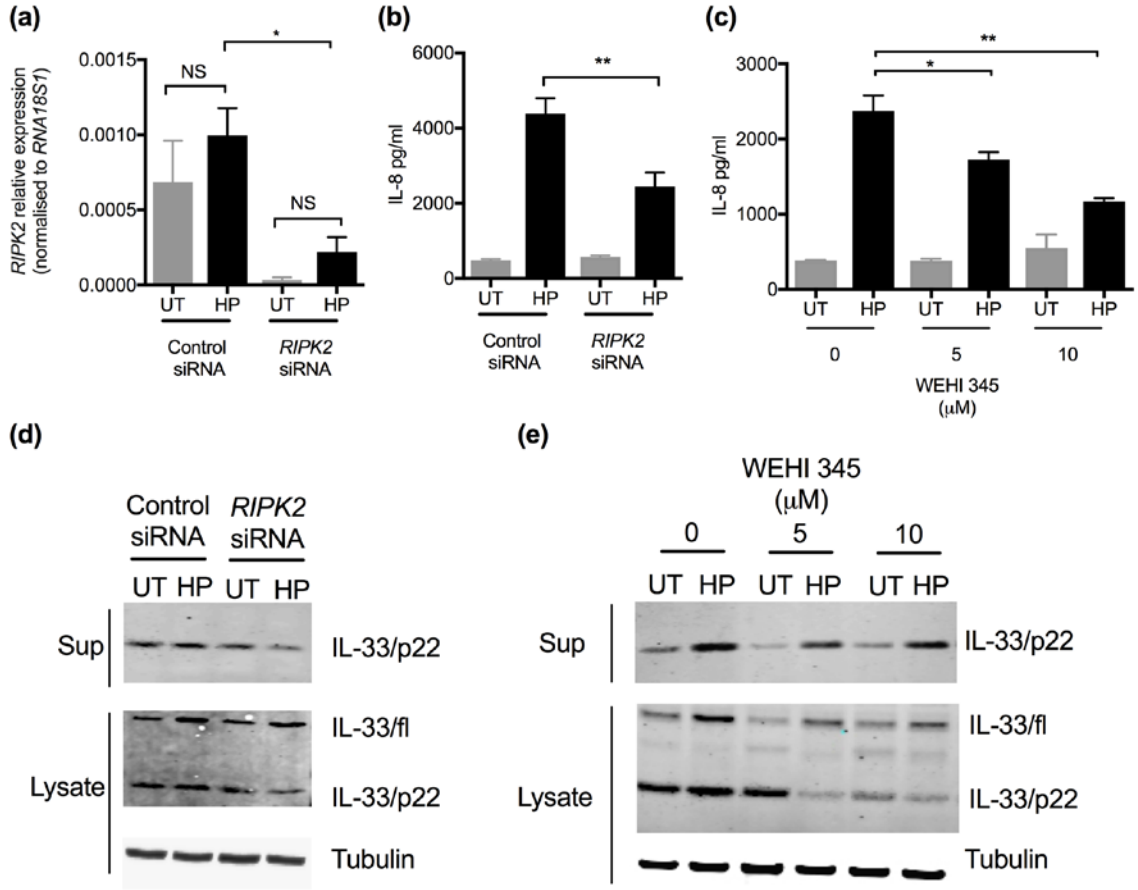

Figure 2. NOD1-mediated IL-33 production and processing in response to *H. pylori* infection are dependent on the NOD1 adaptor molecule, RIPK2.

(a) *RIPK2* gene expression, (b-c) IL-8 and (d-e) IL-33 (full-length and mature form) production in AGS cells transfected with control siRNA or *RIPK2* specific siRNA or pretreated with RIPK2-specific kinase inhibitor WEHI 345 prior to *H. pylori*

stimulation. Data are presented as means ± SEM and are representative of two independent experiments (a-c). ***p*< 0.01, ***p*<0.05. Western blot images (d and e) are representative of 3 independent experiments (n=3). Tubulin served as a loading control.

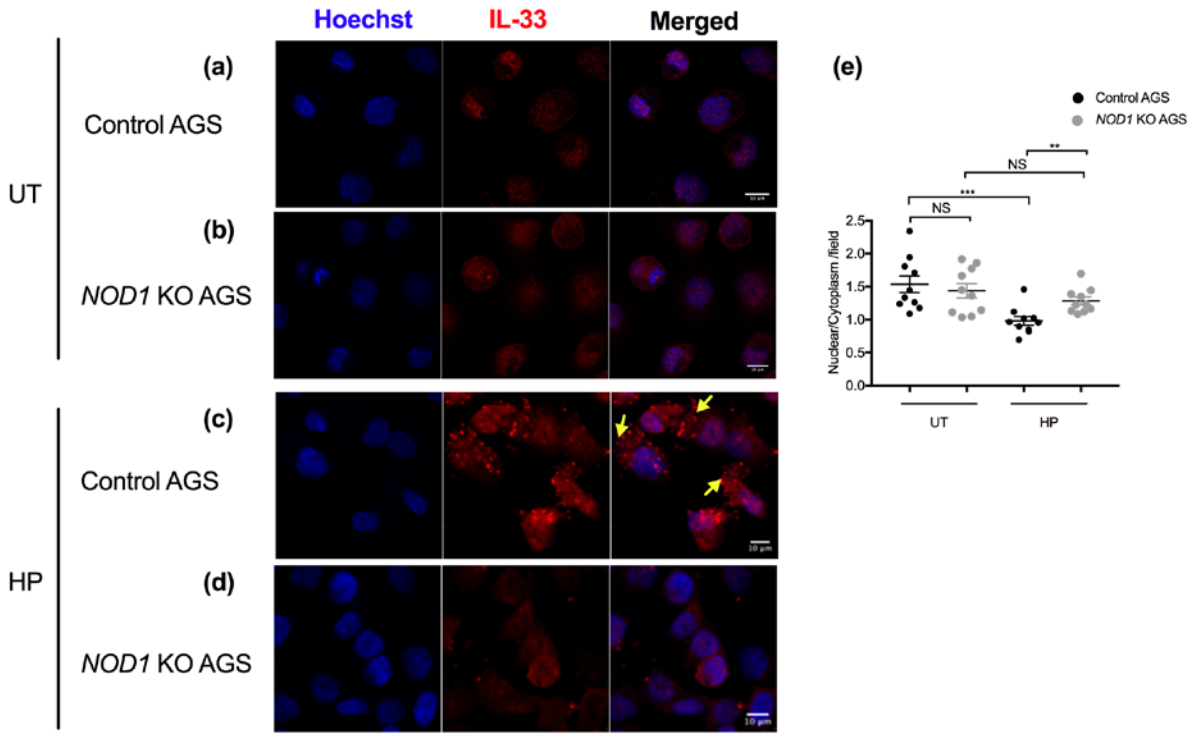

Figure 3. NOD1 mediates loss of nuclear location of IL-33 in human GECs in response to *H. pylori* stimulation.

(a)-(d) Cell nuclei were stained with Hoechst 33342 (blue) and IL-33 (red) detected by immunostaining in AGS control *NOD1* knockout (KO) AGS cells left untreated (a and b) or stimulated with *H. pylori* (c and d) for 24 hrs. Arrows indicate cells displaying loss of nuclear IL-33. Data are representative images of 2 independent experiments. Images were acquired on a confocal microscope with magnification x 200 (scale bar, 5 µm). (e) The nuclear to cytoplasmic ratios of IL-33 staining per field were calculated as described in the Experimental Procedures section. Data are presented as means ± SEM and prepresentative of 2 independent experiments. In each experiment, images were acquired from 10 different fields per treatment group.

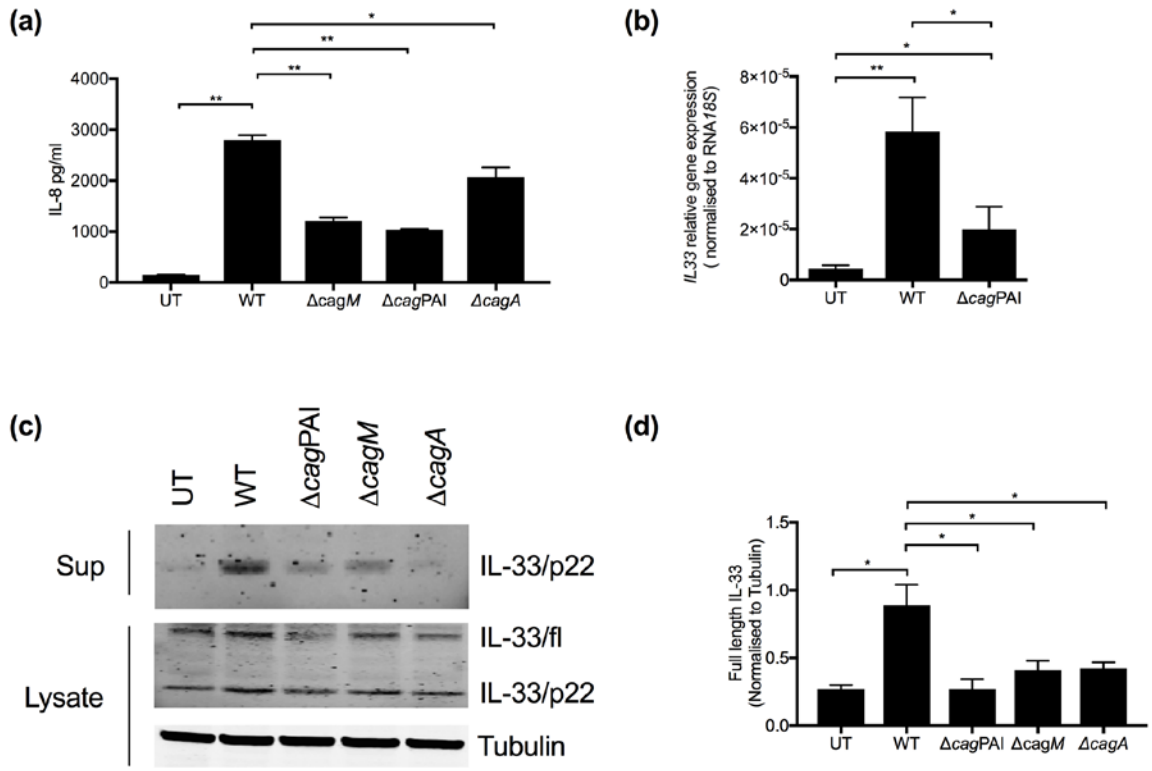

Figure 4. *H. pylori* T4SS and CagA are required for the induction of IL-33 responses in human GECs.

(a) IL-8 production and (b) *IL33* gene expression in AGS cells stimulated with an *H. pylori* wild type strain (WT) or isogenic mutant strains lacking a functional T4SS (ΔCagPAI, ΔCagM) or CagA (ΔCagA). Data are presented as means ± SEM and are representative of three independent experiments (n=3). (c) Full-length or processed IL-33 in AGS cells stimulated with *H. pylori* wild type strain or isogenic mutant strains. (d) Densitometry analysis of blot images in B shows the relative level of full-length IL-33 normalised to Tubulin. Images are representative of results from at least three independent experiments (n>3), and data are presented as the mean ± SEM.

*p< 0.05, **p<0.01.

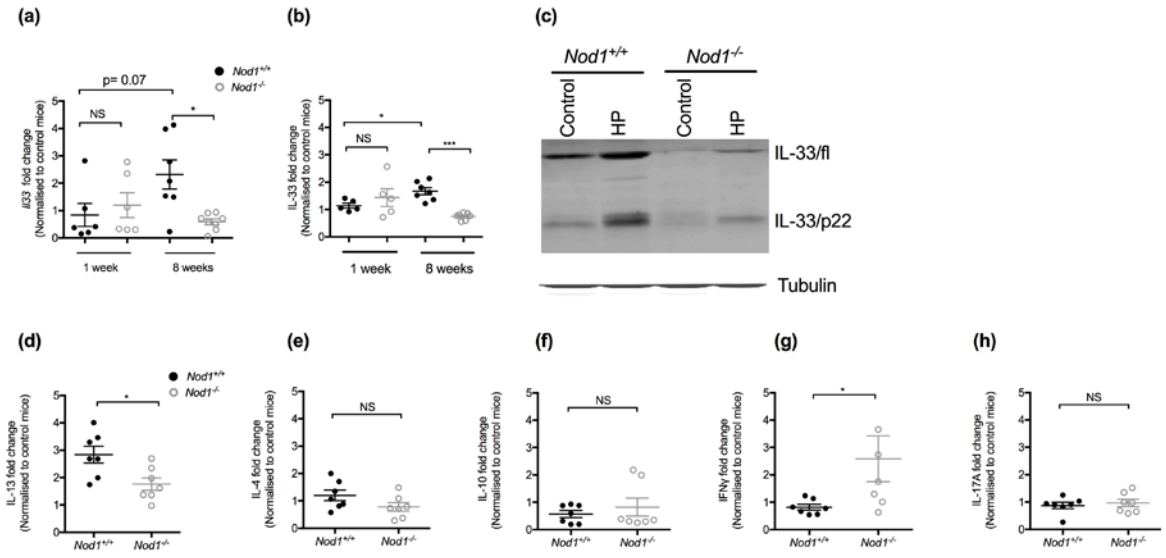

Figure 5. *Nod1*$^{-/-}$ mice display reduced IL-33 production associated with down-regulated IL-13 but up-regulated IFN-γ responses in response to chronic *H. pylori* infection.

(a) Fold changes in *Il33* gene expression and (b) total IL-33 protein levels in gastric homogenates of *Nod1*$^{+/+}$ or *Nod1*$^{-/-}$ mice administered either broth or *H. pylori* for 1 week or 8 weeks. (c) Full-length and mature IL-33 production in the gastric homogenates of *Nod1*$^{+/+}$ or *Nod1*$^{-/-}$ mice at 8 weeks' post-infection. Tubulin was used as a loading control. (d) IL-13, (e) IL-4, (f) IL-10, (g) IFN-γand (h) IL-17 in the culture supernatants of PMA-stimulated splenic cells isolated from mice at 8 weeks' post-infection. Data in (a)-(b), (d)-(h) were normalised to control animals and presented as the means ± SEM. Data are representative of two independent experiments. In each experiment, 4-7 animals per groups per were used (n=4-7). *p<0.05, ** p<0.01, ***p< 0.001, NS not significant.

Supplementary Figure 1. Primary GECs isolated from mice express the epithelial cell-specific marker EpCAM and exhibit NOD1-dependent chemokine responses.

(a) EpCAM and (b) Isotype immunostaining in primary GECs isolated from *Nod1*$^{+/+}$ or *Nod1*$^{-/-}$ mice. Cell nuclei were counterstained with Hoeschst 33342. Representative images were acquired using a Nikon confocal microscope, scale bar = 5 μm, magnification 40X. (c) KC and MIP2 production in the culture supernatants of primary GECs after *H. pylori* stimulation. Data in (c) and (d) are pooled from two independent experiments. * $p<0.05$. (e) Total IL-33 levels in the culture supernatants of mouse GECs (GSM06 cells) treated with ML-130 (5 μM) prior to stimulation with *H. pylori* wild type (26696) or an isogenic mutant (26695 *slt*$^{-}$) at an MOI=10 for 24h. The dashed line on the graph represents the limit of detection.

Supplementary Figure 2. *H. pylori* OMVs induce NOD1 dependent IL-33 production in human gastric epithelial cells.

Full-length and processed IL-33 production after stimulation with BHI broth control or 50 μg of outer membrane vesicles (OMVs) derived from *H. pylori* for 24h. Images are representative of at least 2 independent experiments. Tubulin serves as the loading control for cell lysates.

Supplementary Figure 3. CRISPR/Cas9 targeting of the *NOD1* gene in AGS

cells.

(a) Sequence alignments of a portion of the *NOD1* gene in control and CRISPR/Cas9-mediated *NOD1* knockout AGS cell lines (KO clone#1 and KO clone#2). The gRNA sequences are higlighted in yellow and the protospacer adjacent motif (PAM) is underlied. (b) Predicted translation products in control and *NOD1* knockout AGS clones. (c) *NOD1* gene expression and (d) IL-8 production in control and *NOD1* knockout AGS cell lines after stimulation with the NOD1 agonist, C12-iDAP (10 mg/ml) or *H. pylori* for 24 hrs. Data are presented as the means ± SEM and are representative of 3 independent experiments.

Supplementary Figure 4. TIFA is involved in IL-33 processing but dispensable for the production of full-length IL-33 by human GECs upon *H. pylori* stimulation.

(a) *TIFA* gene expression, (b) IL-8 production and (c) IL-33 production (both full-length and mature forms) in AGS cells transfected with *TIFA*-specific or scramble siRNA prior to *H. pylori* stimulation. Data were presented as means ± SEM and are presentative of 2 independent experiments (a and b). , *p<0.05, ** p<0.01. Western blot images (c) are representative of 2 indpendent experiments (n=2). Tubulin served as a loading control.

Supplementary Table 1: The relative densitometry intensities calculated for each protein band and normalised to Tubulin.

		Lane					
Figure	**Band**	**1**	**2**	**3**	**4**	**5**	**6**
	SUP IL-33/p22	0.29	0.60	0.04	0.27		
	LYS IL-33/fl	0.30	0.69	0.28	0.20		
1c	LYS IL-33/p22	0.14	0.81	0.05	0.08		
	SUP IL-33/p22	0.19	0.21	0.15	0.27	0.32	0.53
	LYS IL-33/fl	0.16	0.21	0.29	0.40	0.43	0.56
1d	LYS IL-33/p22	0.10	0.19	0.24	0.25	0.39	0.40
	SUP IL-33/p22	0.39	0.59	0.40	0.02	0.02	0.13
	LYS IL-33/fl	0.16	0.43	0.06	0.20	0.19	0.27
1e	LYS IL-33/p22	0.19	0.32	0.12	0.16	0.26	0.15
	SUP IL-33/p22	0.36	0.66	0.11	0.12	0.15	0.28
	LYS IL-33/fl	0.25	0.58	0.17	0.31	0.27	0.33
1h	LYS IL-33/p22	0.15	0.30	0.18	0.17	0.41	0.25
	SUP IL-33/p22	0.49	0.63	0.36	0.23		
	LYS IL-33/fl	0.24	0.66	0.21	0.59		
2d	LYS IL-33/p22	0.16	0.34	0.25	0.29		
	SUP IL-33/p22	0.24	0.89	0.08	0.47	0.14	0.58
	LYS IL-33/fl	0.64	1.02	0.26	0.63	0.42	0.56
2e	LYS IL-33/p22	0.73	0.91	0.69	0.13	0.24	0.20
	IL-33/fl	0.69	1.21	0.04	0.44		
5c	IL-33/p22	0.28	1.27	0.19	0.53		

References

[1] Peek RM, Jr., Crabtree JE. Helicobacter infection and gastric neoplasia. The Journal of pathology 2006;208:233-48.
[2] Tran LS, Chonwerawong M, Ferrero RL. Regulation and functions of inflammasome-mediated cytokines in Helicobacter pylori infection. Microbes and infection 2017.
[3] Sayi A, Kohler E, Hitzler I, Arnold I, Schwendener R, Rehrauer H, et al. The CD4+ T cell-mediated IFN-gamma response to Helicobacter infection is essential for clearance and determines gastric cancer risk. Journal of immunology (Baltimore, Md. : 1950) 2009;182:7085-101.
[4] Hitzler I, Kohler E, Engler DB, Yazgan AS, Muller A. The role of Th cell subsets in the control of Helicobacter infections and in T cell-driven gastric immunopathology. Frontiers in immunology 2012;3:142.
[5] Berg DJ, Lynch NA, Lynch RG, Lauricella DM. Rapid development of severe hyperplastic gastritis with gastric epithelial dedifferentiation in Helicobacter felis-infected IL-10(-/-) mice. The American journal of pathology 1998;152:1377-86.
[6] Chen W, Shu D, Chadwick VS. Helicobacter pylori infection: mechanism of colonization and functional dyspepsia Reduced colonization of gastric mucosa by Helicobacter pylori in mice deficient in interleukin-10. Journal of gastroenterology and hepatology 2001;16:377-83.
[7] Smythies LE, Waites KB, Lindsey JR, Harris PR, Ghiara P, Smith PD. Helicobacter pylori-induced mucosal inflammation is Th1 mediated and exacerbated in IL-4, but not IFN-gamma, gene-deficient mice. Journal of immunology (Baltimore, Md. : 1950) 2000;165:1022-9.
[8] Lopetuso LR, Chowdhry S, Pizarro TT. Opposing Functions of Classic and Novel IL-1 Family Members in Gut Health and Disease. Frontiers in immunology 2013;4:181.
[9] Liew FY, Girard JP, Turnquist HR. Interleukin-33 in health and disease. Nature reviews. Immunology 2016;16:676-89.
[10] Molofsky AB, Savage AK, Locksley RM. Interleukin-33 in Tissue Homeostasis, Injury, and Inflammation. Immunity 2015;42:1005-19.
[11] Martin NT, Martin MU. Interleukin 33 is a guardian of barriers and a local alarmin. Nature immunology 2016;17:122-31.
[12] Shahi H, Reiisi S, Bahreini R, Bagheri N, Salimzadeh L, Shirzad H. Association Between Helicobacter pylori cagA, babA2 Virulence Factors and Gastric Mucosal Interleukin-33 mRNA Expression and Clinical Outcomes in Dyspeptic Patients. International journal of molecular and cellular medicine 2015;4:227-34.
[13] Buzzelli JN, Chalinor HV, Pavlic DI, Sutton P, Menheniott TR, Giraud AS, et al. IL33 Is a Stomach Alarmin That Initiates a Skewed Th2 Response to Injury and Infection. Cellular and molecular gastroenterology and hepatology 2015;1:203-21.e3.
[14] Viala J, Chaput C, Boneca IG, Cardona A, Girardin SE, Moran AP, et al. Nod1 responds to peptidoglycan delivered by the Helicobacter pylori cag pathogenicity island. Nature immunology 2004;5:1166-74.

[15] Allison CC, Kufer TA, Kremmer E, Kaparakis M, Ferrero RL. Helicobacter pylori induces MAPK phosphorylation and AP-1 activation via a NOD1-dependent mechanism. Journal of immunology (Baltimore, Md. : 1950) 2009;183:8099-109.
[16] Boonyanugomol W, Chomvarin C, Hahnvajanawong C, Sripa B, Kaparakis-Liaskos M, Ferrero RL. Helicobacter pylori cag pathogenicity island (cagPAI) involved in bacterial internalization and IL-8 induced responses via NOD1- and MyD88-dependent mechanisms in human biliary epithelial cells. PloS one 2013;8:e77358.
[17] Irving AT, Mimuro H, Kufer TA, Lo C, Wheeler R, Turner LJ, et al. The immune receptor NOD1 and kinase RIP2 interact with bacterial peptidoglycan on early endosomes to promote autophagy and inflammatory signaling. Cell host & microbe 2014;15:623-35.
[18] Kaparakis M, Turnbull L, Carneiro L, Firth S, Coleman HA, Parkington HC, et al. Bacterial membrane vesicles deliver peptidoglycan to NOD1 in epithelial cells. Cellular microbiology 2010;12:372-85.
[19] Olofsson A, Vallstrom A, Petzold K, Tegtmeyer N, Schleucher J, Carlsson S, et al. Biochemical and functional characterization of Helicobacter pylori vesicles. Molecular microbiology 2010;77:1539-55.
[20] Baker PJ, De Nardo D, Moghaddas F, Tran LS, Bachem A, Nguyen T, et al. Posttranslational Modification as a Critical Determinant of Cytoplasmic Innate Immune Recognition. Physiological reviews 2017;97:1165-209.
[21] Hasegawa M, Fujimoto Y, Lucas PC, Nakano H, Fukase K, Nunez G, et al. A critical role of RICK/RIP2 polyubiquitination in Nod-induced NF-kappaB activation. The EMBO journal 2008;27:373-83.
[22] Farias R, Rousseau S. The TAK1-->IKKbeta-->TPL2-->MKK1/MKK2 Signaling Cascade Regulates IL-33 Expression in Cystic Fibrosis Airway Epithelial Cells Following Infection by Pseudomonas aeruginosa. Frontiers in cell and developmental biology 2015;3:87.
[23] Kobori A, Yagi Y, Imaeda H, Ban H, Bamba S, Tsujikawa T, et al. Interleukin-33 expression is specifically enhanced in inflamed mucosa of ulcerative colitis. Journal of gastroenterology 2010;45:999-1007.
[24] Correa RG, Khan PM, Askari N, Zhai D, Gerlic M, Brown B, et al. Discovery and characterization of 2-aminobenzimidazole derivatives as selective NOD1 inhibitors. Chemistry & biology 2011;18:825-32.
[25] Grubman A, Kaparakis M, Viala J, Allison C, Badea L, Karrar A, et al. The innate immune molecule, NOD1, regulates direct killing of Helicobacter pylori by antimicrobial peptides. Cellular microbiology 2010;12:626-39.
[26] Inohara N, Koseki T, del Peso L, Hu Y, Yee C, Chen S, et al. Nod1, an Apaf-1-like activator of caspase-9 and nuclear factor-kappaB. The Journal of biological chemistry 1999;274:14560-7.
[27] Gaudet RG, Guo CX, Molinaro R, Kottwitz H, Rohde JR, Dangeard AS, et al. Innate Recognition of Intracellular Bacterial Growth Is Driven by the TIFA-Dependent Cytosolic Surveillance Pathway. Cell reports 2017;19:1418-30.

[28] Gall A, Gaudet RG, Gray-Owen SD, Salama NR. TIFA Signaling in Gastric Epithelial Cells Initiates the cag Type 4 Secretion System-Dependent Innate Immune Response to Helicobacter pylori Infection. mBio 2017;8.
[29] Stein SC, Faber E, Bats SH, Murillo T, Speidel Y, Coombs N, et al. Helicobacter pylori modulates host cell responses by CagT4SS-dependent translocation of an intermediate metabolite of LPS inner core heptose biosynthesis. PLoS pathogens 2017;13:e1006514.
[30] Nachbur U, Stafford CA, Bankovacki A, Zhan Y, Lindqvist LM, Fiil BK, et al. A RIPK2 inhibitor delays NOD signalling events yet prevents inflammatory cytokine production. Nature communications 2015;6:6442.
[31] Kuchler AM, Pollheimer J, Balogh J, Sponheim J, Manley L, Sorensen DR, et al. Nuclear interleukin-33 is generally expressed in resting endothelium but rapidly lost upon angiogenic or proinflammatory activation. The American journal of pathology 2008;173:1229-42.
[32] Moussion C, Ortega N, Girard JP. The IL-1-like cytokine IL-33 is constitutively expressed in the nucleus of endothelial cells and epithelial cells in vivo: a novel 'alarmin'? PloS one 2008;3:e3331.
[33] Inohara N, Koseki T, Lin J, del Peso L, Lucas PC, Chen FF, et al. An induced proximity model for NF-kappa B activation in the Nod1/RICK and RIP signaling pathways. The Journal of biological chemistry 2000;275:27823-31.
[34] Gautier V, Cayrol C, Farache D, Roga S, Monsarrat B, Burlet-Schiltz O, et al. Extracellular IL-33 cytokine, but not endogenous nuclear IL-33, regulates protein expression in endothelial cells. Scientific reports 2016;6:34255.
[35] Carriere V, Roussel L, Ortega N, Lacorre DA, Americh L, Aguilar L, et al. IL-33, the IL-1-like cytokine ligand for ST2 receptor, is a chromatin-associated nuclear factor in vivo. Proceedings of the National Academy of Sciences of the United States of America 2007;104:282-7.
[36] Schmitz J, Owyang A, Oldham E, Song Y, Murphy E, McClanahan TK, et al. IL-33, an interleukin-1-like cytokine that signals via the IL-1 receptor-related protein ST2 and induces T helper type 2-associated cytokines. Immunity 2005;23:479-90.
[37] Cayrol C, Girard JP. The IL-1-like cytokine IL-33 is inactivated after maturation by caspase-1. Proceedings of the National Academy of Sciences of the United States of America 2009;106:9021-6.
[38] Lefrancais E, Roga S, Gautier V, Gonzalez-de-Peredo A, Monsarrat B, Girard JP, et al. IL-33 is processed into mature bioactive forms by neutrophil elastase and cathepsin G. Proceedings of the National Academy of Sciences of the United States of America 2012;109:1673-8.
[39] Philpott DJ, Belaid D, Troubadour P, Thiberge JM, Tankovic J, Labigne A, et al. Reduced activation of inflammatory responses in host cells by mouse-adapted Helicobacter pylory isolates. Cellular microbiology 2002;4:285-96.
[40] Ferrero RL, Ave P, Ndiaye D, Bambou JC, Huerre MR, Philpott DJ, et al. NF-kappaB activation during acute Helicobacter pylori infection in mice. Infection and immunity 2008;76:551-61.

[41] Sawai N, Kita M, Kodama T, Tanahashi T, Yamaoka Y, Tagawa Y, et al. Role of gamma interferon in Helicobacter pylori-induced gastric inflammatory responses in a mouse model. Infection and immunity 1999;67:279-85.
[42] Rad R, Brenner L, Bauer S, Schwendy S, Layland L, da Costa CP, et al. CD25+/Foxp3+ T cells regulate gastric inflammation and Helicobacter pylori colonization in vivo. Gastroenterology 2006;131:525-37.
[43] Gao X, Wang X, Yang Q, Zhao X, Wen W, Li G, et al. Tumoral expression of IL-33 inhibits tumor growth and modifies the tumor microenvironment through CD8+ T and NK cells. Journal of immunology (Baltimore, Md. : 1950) 2015;194:438-45.
[44] Ran FA, Hsu PD, Lin CY, Gootenberg JS, Konermann S, Trevino AE, et al. Double nicking by RNA-guided CRISPR Cas9 for enhanced genome editing specificity. Cell 2013;154:1380-9.
[45] Lee A, O'Rourke J, De Ungria MC, Robertson B, Daskalopoulos G, Dixon MF. A standardized mouse model of Helicobacter pylori infection: introducing the Sydney strain. Gastroenterology 1997;112:1386-97.
[46] Ferrero RL, Wilson JE, Sutton P. Mouse models of Helicobacter-induced gastric cancer: use of cocarcinogens. Methods in molecular biology (Clifton, N.J.) 2012;921:157-73.